

Pacific Journal of Mathematics

PUZZLES IN K -HOMOLOGY OF GRASSMANNIANS

PAVLO PYLYAVSKYY AND JED YANG

PUZZLES IN K -HOMOLOGY OF GRASSMANNIANS

PAVLO PYLYAVSKYY AND JED YANG

Knutson, Tao, and Woodward (2004) formulated a Littlewood–Richardson rule for the cohomology ring of Grassmannians in terms of puzzles. Vakil (2006) and Wheeler and Zinn-Justin (2017) have found additional triangular puzzle pieces that allow one to express structure constants for K -theory of Grassmannians. Here we introduce two other puzzle pieces of hexagonal shape, each of which gives a Littlewood–Richardson rule for K -homology of Grassmannians. We also explore the corresponding eight versions of K -theoretic Littlewood–Richardson tableaux.

1. Introduction

Cohomology rings of flag varieties are a major object of interest in algebraic geometry, see [Fulton 1984; Manivel 2001] for an exposition. Perhaps the most well-studied and well-understood examples are the cohomology rings of Grassmannians, with a distinguished basis of Schubert classes. A *Littlewood–Richardson rule* is a combinatorial way to compute the structure constants for this basis. Equivalently, those are the same structure constants $c_{\lambda\mu}^{\nu}$ with which certain symmetric functions — *Schur functions* s_{λ} — multiply: $s_{\lambda}s_{\mu} = \sum_{\nu} c_{\lambda\mu}^{\nu}s_{\nu}$. In their groundbreaking work Knutson, Tao, and Woodward [Knutson and Tao 1999; Knutson et al. 2004] introduced *puzzles*, which allow for a powerful formulation of the Littlewood–Richardson rule. Puzzles are tilings of triangular boards with specified boundary conditions by a set of tiles shown in Figure 1. Using puzzles Knutson, Tao, and Woodward studied the faces of the Klyachko cone.

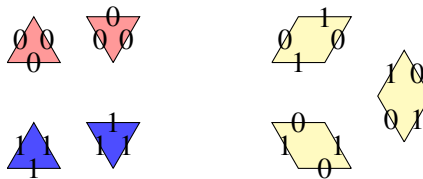


Figure 1. The Knutson–Tao–Woodward tiles.

MSC2010: primary 05E15; secondary 14M15, 52C20.

Keywords: puzzles, hexagon, tiling, K -theory, Grassmannian, Littlewood–Richardson coefficient.

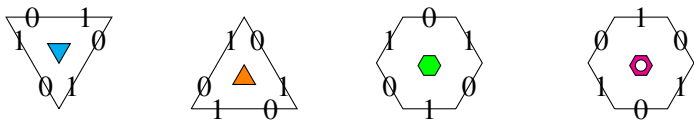


Figure 2. The four K -theoretic tiles.

There is a cohomology theory for each one-dimensional group law [Hazewinkel 1978; Lenart and Zainoulline 2017]. For the additive group law $x \oplus y = x + y$ one has the usual cohomology, while the multiplicative group law $x \oplus y = x + y + xy$ gives the K -theory. K -theory of Grassmannians was extensively studied, starting with the works of Lascoux and Schützenberger. In [Lascoux and Schützenberger 1982] they introduced the *Grothendieck polynomials* as representatives of K -theory classes of structure sheaves of Schubert varieties. Fomin and Kirillov [1995] studied those from combinatorial point of view, introducing the *stable Grothendieck polynomials* G_λ . Stable Grothendieck polynomials are symmetric power series that form a rather precise K -theoretic analogue of Schur functions: their multiplicative structure constants are the same as those for classes of the structure sheaves of Schubert varieties in the corresponding K -theory ring.

The first K -theoretic Littlewood–Richardson rule was obtained by Buch [2002]. Vakil [2006] has extended puzzles to K -theory, giving a puzzle version of the rule. His extension works by adding a single additional tile to the set of tiles from the work of Knutson, Tao and Woodward [Knutson et al. 2004]. Later, Wheeler and Zinn-Justin [2017] found an alternative K -theoretic tile, that gives the structure constants of dual K -theory in an appropriate sense. Both Vakil and Wheeler–Zinn-Justin tiles have triangular shape and can be seen in Figure 2.

In this work we present *two new tiles*, adding either one of which to the standard collection allows one to recover structure constants of the Schubert basis in the K -homology ring of the Grassmannians, as studied by Lam and Pylyavskyy [2007]. Equivalently, the corresponding puzzles produce a combinatorial rule for the *co-product* structure constants of the stable Grothendieck polynomials. The first such rule was obtained by Buch [2002]. The tiles have *hexagonal shape* and can be seen in Figure 2.

The paper proceeds as follows. In Section 2 we recall the known results on the cohomology ring of Grassmannians, including tableaux and puzzles formulations of the Littlewood–Richardson rule. In Section 3 we recall the K -theoretic version of the story, and state our main results regarding the two new hexagonal tiles. We also systematize the eight different tableaux formulations of the K -theoretic Littlewood–Richardson rule, some of which are new. The proofs are postponed to Section 4. In Section 5 we conclude with remarks, including the relation of our work to that of Pechenik and Yong [2017] on genomic tableaux.

2. Puzzles and tableaux

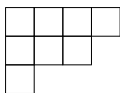
2A. Cohomology of Grassmannians. Let $\text{Gr}(k, n)$ be the variety of k -dimensional subspaces of \mathbb{C}^n . Recall that a *partition* $\lambda = (\lambda_1, \lambda_2, \dots, \lambda_k)$ is a weakly decreasing sequence $\lambda_1 \geq \lambda_2 \geq \dots \geq \lambda_k \geq 0$ of finitely many nonnegative integers. Restrict to the set of partitions with k parts and with $\lambda_1 \leq n - k$. Fix a complete flag $0 = V_0 \subset V_1 \subset \dots \subset V_n = \mathbb{C}^n$, with $\dim(V_i) = i$. The *Schubert variety* in $\text{Gr}(k, n)$ associated to λ is the set

$$X_\lambda = \{W \in \text{Gr}(k, n) \mid \dim(W \cap V_{n+k+i-\lambda_i}) \geq i, \forall i \in [k]\}.$$

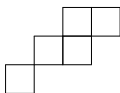
The associated classes $[X_\lambda]$ in the cohomology ring $H_*(\text{Gr}(k, n), \mathbb{Z})$ are known to form a basis, with the structure constants $c_{\lambda\mu}^\nu$ called *Littlewood–Richardson coefficients*:

$$[X_\lambda] \cdot [X_\mu] = \sum_{\nu} c_{\lambda\mu}^\nu [X_\nu].$$

Littlewood–Richardson coefficients can also be described in the following elementary way. The Young diagram, or simply, *diagram*, of a partition λ is a collection of boxes, top and left justified, with λ_i boxes in row i . For example, this is the diagram of the partition $\lambda = (4, 3, 1)$:



If λ is a partition whose diagram fits inside that of partition ν , the *skew diagram* of shape ν/λ is the diagram consisting of the boxes of the diagram of ν outside that of λ . For example, the following is the diagram of $(4, 3, 1)/(2, 1)$:



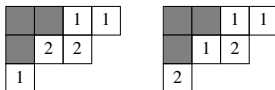
Given a (possibly skew) diagram and a set V , a V -*tableau* T is a filling of the boxes with values in V . If V is omitted, it is understood that V is the positive integers. The *shape* of T , denoted $\text{shape}(T)$, is the shape of the diagram. We say that T is *semistandard* if the values are weakly increasing from left to right in rows and strictly increasing from top to bottom in columns. The *reverse row word* of T , denoted $\text{row}(T)$, is the sequence of values of T , read row by row, top to bottom, right to left. For example,

$$T = \begin{array}{ccccc} & & & 1 & 1 \\ & & 2 & 2 & \\ 1 & & & & \end{array}$$

is a semistandard tableau with $\text{shape}(T) = (4, 3, 1)/(2, 1)$ and $\text{row}(T) = 11221$.

$$s_\lambda(x) = \sum_T x^T,$$
$$S_\lambda S_\mu = \sum_\nu C_{\lambda\mu}^\nu S_\nu.$$

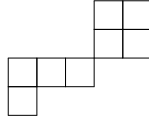
Example 2.2. Let $\lambda = (2, 1)$, $\mu = (3, 2)$, and $\nu = (4, 3, 1)$ in the following examples. The following are the (only) two ways to fill according to the Littlewood–Richardson rule.



¹For example, if $w = \text{row}(T)$, then in the monomial x^T , the exponent of x_i is m_i .

This shows that $c_{\lambda\mu}^v = 2$. For visual purposes, we gray out the boxes corresponding to λ instead of removing them. (This will be useful later when we temporarily write numbers in removed boxes.)

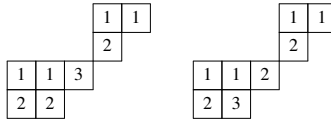
Given two partitions λ and μ , let the \oplus diagram of shape $\mu \oplus \lambda$ be obtained by putting the diagrams of μ and λ corner to corner, with μ to the lower left and λ to the upper right. For example,



is a diagram of shape $(3, 1) \oplus (2, 2)$.

Theorem 2.3 (Littlewood–Richardson rule, \oplus version). *For partitions λ, μ, v such that $|v| = |\lambda| + |\mu|$, the coefficient $c_{\lambda\mu}^v$ is the number of semistandard ballot tableaux of shape $\mu \oplus \lambda$ and content v .*

Example 2.4. We continue with λ, μ, v from the example above. The following are the two corresponding fillings using the \oplus version of the Littlewood–Richardson rule.



These are displayed in the same order under the bijection that is described in later sections.

Of course, any \oplus diagram $\mu \oplus \lambda$ is also a skew diagram of shape

$$(\lambda_1 + \mu_1, \dots, \lambda_k + \mu_1, \mu_1, \dots, \mu_k).$$

Nevertheless, we think of these classes of shapes separately, since we will have pairs of tableaux rules, one involving shape v/λ and one involving shape $\mu \oplus \lambda$. We refer to v/λ as skew shape (and use grayed out boxes) and refer to $\mu \oplus \lambda$ as \oplus shape (without using grayed out boxes).

2C. Puzzle version of the Littlewood–Richardson rule. Let $n \geq k$ be positive integers. Refer to the partition of k rows of length $n - k$ as the *ambient rectangle*. From now on, we consider only partitions whose diagrams fit inside this ambient rectangle. (To consider bigger partitions, simply specify a larger ambient rectangle.) On the lower right boundary of a partition inside the ambient rectangle, write a 0 on each horizontal edge and a 1 on each vertical edge (see Figure 3). A binary string of length n with k ones and $n - k$ zeros is obtained by reading these numbers from top right to bottom left.

Here we consider tilings on the triangular lattice. Knutson, Tao, and Woodward [Knutson et al. 2004] introduced the following *puzzle pieces* (see Figure 4).

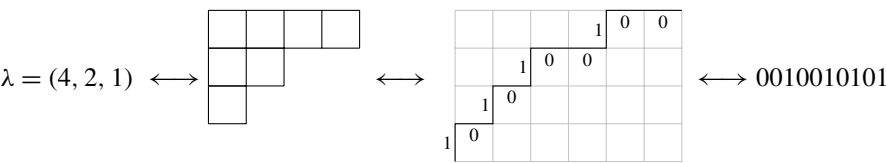


Figure 3. Bijection between partitions, Young diagrams, and binary strings; $n = 10, k = 4$.

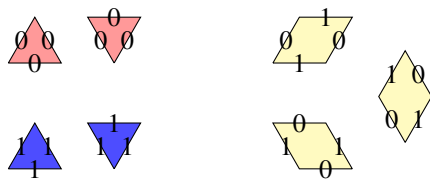


Figure 4. Puzzle pieces.

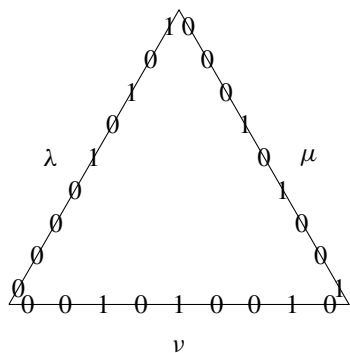


Figure 5. Boundary $\Delta_{\lambda\mu}^{\nu}$ with $\lambda = (2, 1, 0)$, $\mu = (3, 2, 0)$, and $\nu = (4, 3, 1)$.

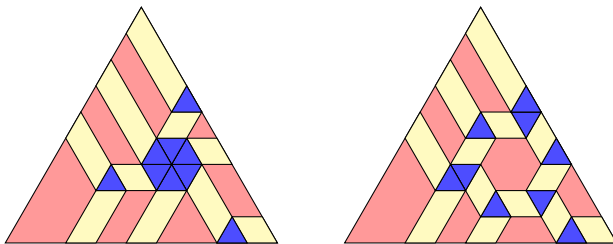
- 0-triangle: unit triangle with edges labeled by 0, two rotations;
- 1-triangle: unit triangle with edges labeled by 1, two rotations; and
- rhombus: formed by gluing two adjacent unit triangles together, with edges labeled by 0 if clockwise of an acute angle and 1 if clockwise of an obtuse angle, three rotations.

A *tiling* is an assembly of (lattice) translated copies of tiles, where edge labels of adjacent tiles must match. We are interested in tiling an upright triangular region $\Delta_{\lambda\mu}^{\nu}$ whose boundary labels of the left, right, and bottom sides, read left-to-right, are the binary strings corresponding to λ , μ , and ν (see Figure 5).

Littlewood–Richardson coefficients can be calculated by counting puzzle tilings:

Theorem 2.5 [Knutson et al. 2004]. Suppose λ, μ, ν are partitions fitting inside an $(n - k) \times k$ ambient rectangle, with $|\nu| = |\lambda| + |\mu|$. The number of puzzle tilings with boundary $\Delta_{\lambda\mu}^\nu$ is $c_{\lambda\mu}^\nu$.

Example 2.6. Continuing with the running example from the previous section, since $c_{\lambda\mu}^\nu = 2$, there are two tilings of $\Delta_{\lambda\mu}^\nu$:



Here and subsequently, some edges (namely, the edges within a region of 0-triangles and the 1-edges of a sequence of rhombi) are omitted to suggest the structure of puzzle tilings.

The bijection between the tableau rule and the puzzle rule can be seen with Tao's "proof without words" (see [Vakil 2006]). More details of this bijection is given when we generalize it in Section 4B. The reader is encouraged to use Zinn-Justin's puzzle viewer [2016] to aid in visualizing these puzzles.

3. K -theoretic puzzles and tableaux

In this section, we discuss four K -theoretic analogues of the Littlewood–Richardson coefficients. These coefficients can be calculated using four puzzle rules and eight tableaux rules.

3A. K -theory and K -homology of Grassmannians. Just as in the case of ordinary cohomology, the classes of the structure sheaves \mathcal{O}_{X_λ} form a basis for the Grothendieck ring $K^\circ(\text{Gr}(k, n))$. The associated structure constants $c_{\lambda\mu}^\nu$ are given by

$$[\mathcal{O}_{X_\lambda}] \cdot [\mathcal{O}_{X_\mu}] = \sum_{\nu} c_{\lambda\mu}^\nu [\mathcal{O}_{X_\nu}],$$

and generalize the usual Littlewood–Richardson coefficients in the sense that one recovers the latter for triples λ, μ, ν such that $|\lambda| + |\mu| = |\nu|$. An elementary construction of those structure constants also exists, with the K -theoretic analogue of a Schur function s_λ being the *single stable Grothendieck polynomial* G_λ given by the formula

$$G_\lambda = \sum_T (-1)^{|T| - |\lambda|} x^T,$$

where the sum runs over all semistandard set-valued tableaux T of shape λ , and $|T|$ is the length of $\text{row}(T)$. The equivalence of this definition to other definitions is established by Buch [2002].

In addition to the K -theory ring $K^\circ(\text{Gr}(k, n))$ one can also consider a K -homology ring $K_\circ(\text{Gr}(k, n))$. The classes of the ideal sheaves \mathcal{I}_{X_λ} of the boundary of the Schubert varieties X_λ form a basis in this ring. It turns out that this basis and the basis of classes of structure sheaves \mathcal{O}_{X_λ} in $K^\circ(\text{Gr}(k, n))$ are dual in a precise sense. The structure constants $d_{\lambda\mu}^v$ of the classes $[\mathcal{I}_{X_\lambda}]$ are given by

$$[\mathcal{I}_{X_\lambda}] \cdot [\mathcal{I}_{X_\mu}] = \sum_v d_{\lambda\mu}^v [\mathcal{I}_{X_v}],$$

and also constitute a generalization of the classical Littlewood–Richardson coefficients, recovering the latter in the case $|\lambda| + |\mu| = |v|$. We refer the reader to [Lam and Pylyavskyy 2007] for details. The same reference also gives a definition of *dual stable Grothendieck polynomials* g_λ , which generalize Schur functions in the sense of their structure constants being exactly the $d_{\lambda\mu}^v$.

One can recover the $d_{\lambda\mu}^v$ directly from the stable Grothendieck polynomials G_λ however, as follows. Buch has showed that the linear span of $\{G_\lambda\}_\lambda$ inherits from symmetric functions the structure of a bialgebra, with product given by

$$G_\lambda G_\mu = \sum_v (-1)^{|v| - |\lambda| - |\mu|} c_{\lambda\mu}^v G_v$$

and coproduct Δ given by

$$\Delta(G_v) = \sum_{\lambda, \mu} (-1)^{|v| - |\lambda| - |\mu|} d_{\lambda\mu}^v G_\lambda \otimes G_\mu.$$

In other words, the product structure constants $c_{\lambda\mu}^v$ for the G_λ are the coproduct structure constants for the g_λ , and vice versa.

It turns out that

$$c_{\lambda\mu}^v = 0 \quad \text{when } |v| < |\lambda| + |\mu| \quad \text{and} \quad d_{\lambda\mu}^v = 0 \quad \text{when } |v| > |\lambda| + |\mu|.$$

So we might as well restrict the first and second sums to the cases where $|v| \geq |\lambda| + |\mu|$ and $|v| \leq |\lambda| + |\mu|$, respectively. Unlike the classical case, this does not immediately show that the sums are finite, but indeed they are (Corollaries 5.5 and 6.7 of [Buch 2002]).

As we mentioned above, when $|v| = |\lambda| + |\mu|$, the number $c_{\lambda\mu}^v$ is indeed the classical Littlewood–Richardson coefficient described in previous sections. Since this is the only case where the classical $c_{\lambda\mu}^v$ is possibly nonzero, by an abuse of notation, we use the same symbol to denote both. It is therefore paramount to require $|v| = |\lambda| + |\mu|$ when discussing $c_{\lambda\mu}^v$ in the classical case.

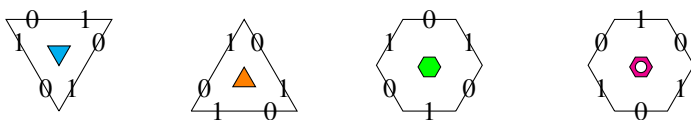


Figure 6. Four additional puzzle pieces.

The following slight variants of $c_{\lambda\mu}^v$ and $d_{\lambda\mu}^v$ arise naturally in the study of puzzles. Let $\tilde{G}_\lambda = G_\lambda \cdot (1 - G_1)$. Define $\tilde{c}_{\lambda\mu}^v$ as the unique numbers such that

$$\tilde{G}_\lambda \cdot \tilde{G}_\mu = \sum_v (-1)^{|v| - |\lambda| - |\mu|} \tilde{c}_{\lambda\mu}^v \tilde{G}_v.$$

We again restrict to $|v| \geq |\lambda| + |\mu|$, the only time when $\tilde{c}_{\lambda\mu}^v$ is possibly nonzero. The meaning of the \tilde{G}_λ in that they also represent ideal sheaves of Schubert varieties in certain rings is explained in [Wheeler and Zinn-Justin 2017].

Finally, let $\tilde{d}_{\lambda\mu}^v$ be given by $d_{\lambda'\mu'}^v$, where λ' is the transpose of λ , i.e., mirror the diagram of λ across the line $x + y = 0$. Since the number of boxes is preserved, the only time $\tilde{d}_{\lambda\mu}^v$ is possibly nonzero is when $|v| \leq |\lambda| + |\mu|$. The $\tilde{d}_{\lambda\mu}^v$ form the same collection of structure constants as the $d_{\lambda\mu}^v$, just indexed differently.

3B. The four K -theoretic puzzles. Consider the puzzle pieces shown in Figure 6.

We refer to these puzzle pieces using the corresponding pictograms shown in the figure. If X is (the pictogram of) an additional puzzle piece, an X -puzzle is a puzzle tiling where, in addition to the usual puzzle pieces, translated copies of X can be used. There are known interpretations of \blacktriangledown -puzzles and \blacktriangle -puzzles.

Theorem 3.1 [Vakil 2006]. *Suppose λ, μ, v are partitions fitting inside an $(n-k) \times k$ ambient rectangle, with $|v| \geq |\lambda| + |\mu|$. The number of \blacktriangledown -puzzle tilings with boundary $\Delta_{\lambda\mu}^v$ is $c_{\lambda\mu}^v$.*

Theorem 3.2 [Wheeler and Zinn-Justin 2017]. *Suppose λ, μ, v are partitions fitting inside an $(n-k) \times k$ ambient rectangle, with $|v| \geq |\lambda| + |\mu|$. The number of \blacktriangle -puzzle tilings with boundary $\Delta_{\lambda\mu}^v$ is $\tilde{c}_{\lambda\mu}^v$.*

We establish interpretations of \bullet -puzzles and \circ -puzzles.

Theorem 3.3. *Suppose λ, μ, v are partitions fitting inside an $(n-k-1) \times k$ ambient rectangle,² with $|v| \leq |\lambda| + |\mu|$. The number of \bullet -puzzle tilings with boundary $\Delta_{\lambda\mu}^v$ is $d_{\lambda\mu}^v$.*

Theorem 3.4. *Suppose λ, μ, v are partitions fitting inside an $(n-k) \times (k-1)$ ambient rectangle, with $|v| \leq |\lambda| + |\mu|$. The number of \circ -puzzle tilings with boundary $\Delta_{\lambda\mu}^v$ is $\tilde{d}_{\lambda\mu}^v$.*

²For technical reasons, we require partitions to be slightly smaller. See Section 5A.

3C. The eightfold way. Like the classical case, where the puzzle rule corresponds to a pair of tableau rules (involving diagrams of shapes ν/λ and $\mu \oplus \lambda$, respectively), we describe four pairs of K -tableau rules corresponding to the four K -puzzle rules.

A *set-valued tableau* is a V -tableau where V consists of nonempty subsets of $\{1, \dots, k\}$. To understand the semistandard condition in this context, we agree that for $A, B \in V$, A is (strictly) less than B if $\max A$ is (strictly) less than $\min B$. When forming the reverse row word, a value $A \in V$ is expanded as the numbers in the set A , written from largest to smallest.

Buch [2002] gives a combinatorial rule for calculating the K -theory Littlewood–Richardson coefficient $c_{\lambda\mu}^{\nu}$ by counting certain set-valued tableaux of \oplus shape.

Theorem 3.5 (▼ rule, \oplus version). *The coefficient $c_{\lambda\mu}^{\nu}$ is the number of semistandard ballot set-valued tableaux of shape $\mu \oplus \lambda$ and content ν .*

To describe the skew version of the K -theory rule, we consider a new kind of tableaux. A *circle tableau* T is a V -tableau where V consists of $\{1, \dots, k\}$ and the *circled* numbers $\{\textcircled{1}, \dots, \textcircled{k}\}$.

We say T is a *right* (resp. *left*) circle tableau if each \textcircled{i} is the rightmost (resp. leftmost) i or \textcircled{i} in its row. (In other words, for each i , only the rightmost (resp. leftmost) i in a row is optionally circled.) Moreover, circled values may only occur in the bottom k rows (that is, anywhere in shape ν/λ , bottom half in shape $\mu \oplus \lambda$).

We say T is *semistandard* if it is semistandard when the circled values are treated as if they are not circled. Its *content* is $\text{content}(w)$ where w is $\text{row}(T)$ with the circled values omitted.

Let w be an initial segment of $\text{row}(T)$. If w ends with \textcircled{i} , replace it with an uncircled $i + 1$. Remove all other circled entries. Call the result the *incremented erasure* of w . Analogously, call the result the *unincremented erasure* of w if the final \textcircled{i} is replaced with an uncircled i instead. We say that a right (left) circle tableau is *ballot* if all its incremented (unincremented) erasures are ballot.

Pechenik and Yong [2017] give a combinatorial rule for calculating the K -theory Littlewood–Richardson coefficient $c_{\lambda\mu}^{\nu}$ by counting certain *genomic* tableaux of skew shape. We give an equivalent formulation (see Section 5C) here in terms of circle tableaux.

Theorem 3.6 (▼ rule, skew version). *The coefficient $c_{\lambda\mu}^{\nu}$ is the number of semistandard ballot right circle tableaux of shape ν/λ and content μ .*

An *outer corner* of (the diagram of) a partition μ is a box whose addition results in a diagram of a partition.

Theorem 3.7 (▲ rule, \oplus version). *The coefficient $\tilde{c}_{\lambda\mu}^{\nu}$ is the number of semistandard ballot set-valued tableaux of shape $\mu^+ \oplus \lambda$ and content ν , where μ^+ is μ with some number (possibly zero) of its outer corners added.*

Theorem 3.8 (▲ rule, skew version). *The coefficient $\tilde{c}_{\lambda\mu}^v$ is the number of semistandard ballot left circle tableaux of shape v/λ and content μ .*

Recall that a circle tableau of shape $\mu \oplus \lambda$ does not have circles in the rows corresponding to λ .

Theorem 3.9 (◆ rule, \oplus version). *The coefficient $d_{\lambda\mu}^v$ is the number of semistandard ballot right circle tableaux of shape $\mu \oplus \lambda$ and content v .*

An *inner corner* of (the diagram of) a partition λ is a box whose removal results in a diagram of a partition.

Theorem 3.10 (◆ rule, skew version). *The coefficient $d_{\lambda\mu}^v$ is the number of semistandard ballot set-valued tableaux of shape v/λ^- and content μ , where λ^- is λ with some number (possibly zero) of its inner corners removed.*

A circle tableau of shape $\mu \oplus \lambda$ is *limited* if it has no ① in row i of the bottom half for any i .

Theorem 3.11 (⬢ rule, \oplus version). *The coefficient $\tilde{d}_{\lambda\mu}^v$ is the number of limited semistandard ballot left circle tableaux of shape $\mu \oplus \lambda$ and content v .*

Theorem 3.12 (⬢ rule, skew version). *The coefficient $\tilde{d}_{\lambda\mu}^v$ is the number of semistandard ballot set-valued tableaux of shape v/λ and content μ .*

Note that the limited condition present in the \oplus version of the ⬢ rule does not appear in the skew version. Instead, the limited condition arises implicitly in the skew version of the ▼ rule (Theorem 3.6). In that case, the ballot condition implies the limited condition. See Section 4D for details.

4. Proofs

4A. Proof of Theorem 3.10. Given a sequence $w = (w_1, \dots, w_r)$ and an interval $[a, b]$, let $w|_{[a,b]}$ be the sequence obtained by shifting the numbers down to the interval $[1, b - a + 1]$ by subtracting $a - 1$ from each number w_i in the range $[a, b]$ (and omitting numbers that are out of the range).

Theorem 4.1 [Buch 2002]. *The coefficient $d_{\lambda\mu}^v$ is the number of semistandard set-valued tableaux T of shape v with content $(\lambda, \mu) = (\lambda_1, \lambda_2, \dots, \lambda_k, \mu_1, \dots, \mu_k)$, such that $\text{row}(T)|_{[1,k]}$ and $\text{row}(T)|_{[k+1,2k]}$ are both ballot.*

For notational convenience, local to this proof only, a *Buch tableau* is one described in Theorem 4.1. and a *◆ tableau* is one described in Theorem 3.10. There is a simple bijection between Buch tableaux and ◆ tableaux.

Indeed, let T be a ◆ tableau. Increase each number in T by k . Extend the shape of T to v by filling in the first λ_i boxes of T with i in row i . The result is clearly a Buch tableau.



Figure 7. Left: a beam of length 3. Right: three beams of length 1.

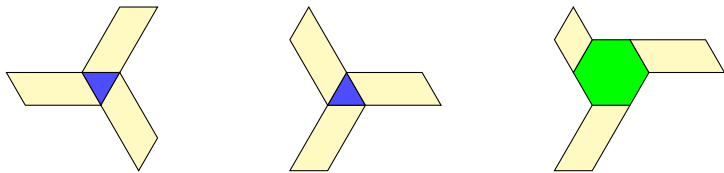


Figure 8. All the ways beams can meet.

Conversely, let T be a Buch tableau. It is easy to see that, as T is semistandard and $\text{row}(T)_{|[1,k]}$ is ballot, the λ_i occurrences of i are exactly in the first λ_i boxes of row i . Remove these “small” numbers. A remaining “big” number in row i cannot be in the first $\lambda_i - 1$ boxes, since the λ_i -th box contained a small number. It can be in the λ_i -th box only if the λ_i -th box in the next row did not contain a small number. In other words, only if this box is an inner corner of λ . We therefore conclude that the shape of the remaining tableau is ν/λ with some (possibly zero) inner corners of λ added. Decrease k from all the remaining numbers to obtain a \blacklozenge tableau.

This concludes the proof of [Theorem 3.10](#).

4B. Proof of [Theorem 3.3](#). We prove [Theorem 3.3](#) by establishing a bijection between \blacklozenge -puzzles and the tableaux described in [Theorem 3.10](#). For notational convenience, we do so by considering an example when $k = 4$. The general case is similar.

First, we consider the structure of a generic \blacklozenge -puzzle. In a tiling, the rhombi form *beams*, a sequence of rhombi adjacent by their 1-edges. The number of rhombi in the beam is its *length*. If beams are adjacent to each other because some rhombi are adjacent by their 0-edges, we consider the beams as separate beams of width one (see [Figure 7](#)). Otherwise, three beams can meet at a 1-triangle or a \blacklozenge , as in [Figure 8](#).

If no \blacklozenge piece is used, the structure is simple, and can be seen in Tao’s “proof without words” (see [\[Vakil 2006\]](#)). From the bottom boundary, each 1-edge is adjacent to an *upward* beam (possibly of zero length). The top of each upward beam must be an upright 1-triangle. The left and right side of the 1-triangle are each adjacent to a *leftward* and a *rightward* beam, respectively. A leftward beam terminates either at the left boundary or the right side of an upside-down 1-triangle. Similarly, a rightward beam terminates at the right boundary or the left side of an

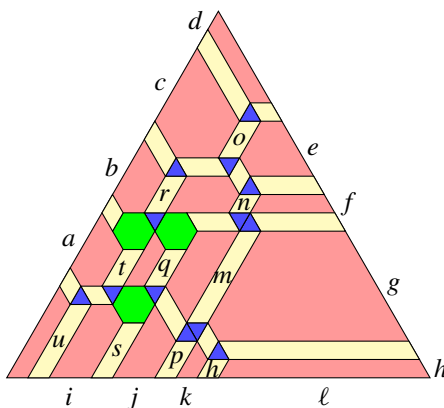






Figure 9. An example tiling.

upside-down 1-triangle. These upside-down 1-triangles have upward beams on their top edges. The rest of the puzzle is filled with 0-triangles.

Now we consider adding in the  piece (see Figure 9). Since the  piece has 1-edges in the same orientation as the upright 1-triangle, it can be placed on top of an upright beam to replace an upright 1-triangle. It also must have a leftward and a rightward beam adjacent to its two other 1-edges. As compared to using a 1-triangle instead of the  piece, the length of the leftward beam is decreased by one, and the rightward beam is shifted up by one.

In Figure 9, the upright beams have labels. We refer to the beam with label x as the x -beam. By abuse of notation, we also let x denote the length (that is, the number of rhombi) of the x -beam. For each x -beam, set x' to x . Increment x' by one if the x -beam is capped with a  on top (as opposed to a triangle). In the example in the figure, t' , q' , and s' are the ones that are incremented. The boundary also has some length labels. We use the same labels as those in Tao's "proof without words."

Note that these numbers completely determine the tiling. Indeed, let us describe a process to assemble such a tiling based on the numbers. Place (the rhombi of) the bottom beams according to their lengths (e.g., u , s , p , and h). Place 1-triangles or hexagons on top of them based on whether $x' = x$ or not. Extend the leftmost leftward beam and the rightmost rightward beam to the boundary. In the middle, extend each pair of leftward and rightward beams until they meet each other. That is the unique position to place an upside-down 1-triangle. If we had k beams at the bottom, there are now $k - 1$ upside-down 1-triangles. Repeat the process according to the lengths of the second level of upward beams (e.g., t , q , and m). The puzzle can be built level by level, each time with one fewer upward beam. Finally, fill the rest of the puzzle with 0-triangles.

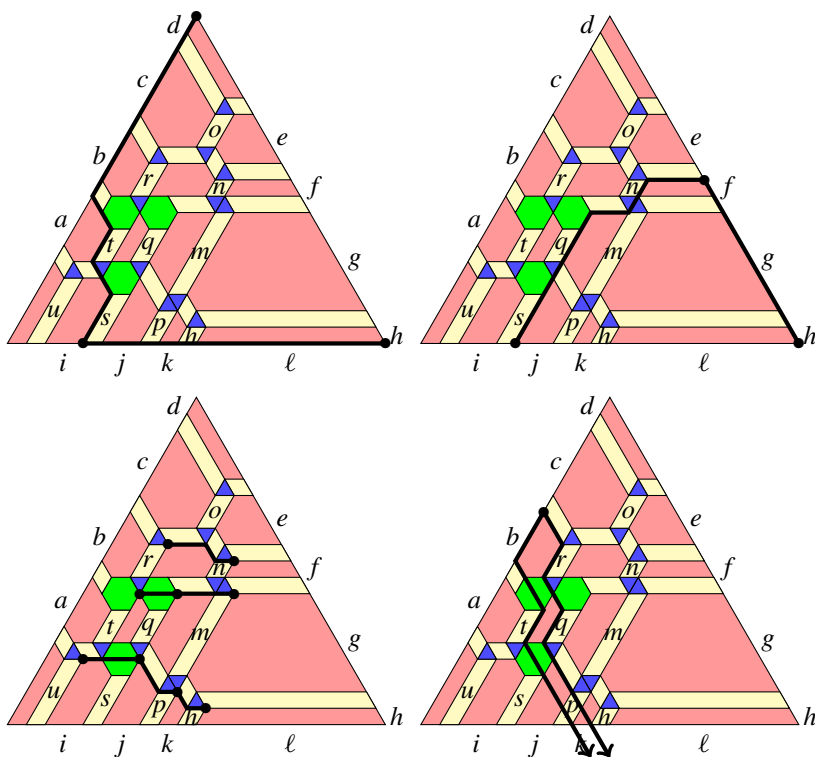


Figure 10. Inequalities from puzzles.

In general, ① can only be written in the boxes corresponding to the *inner corners* of λ .

Finally, uncircle the circled numbers in T . Since circled numbers either share boxes with uncircled numbers or occur in the inner corners of λ , what we get is a set-valued tableau of shape ν/λ^- , where λ^- is λ with some inner corners removed. This concludes one direction of the bijection.

Reversing the bijection is straightforward. First, we reverse the last step. Let T' be a set-valued tableau of shape ν/λ^- and content μ , where λ^- is λ with some of its inner corners removed. Circle all the numbers in boxes corresponding to inner corners of λ and all but the smallest number in each of the boxes corresponding to ν/λ . This tableau with circles is in fact T as described in the middle of the bijection above. Indeed, as T' is ballot, the numbers appearing in row i are all at most i . Also, if we were to get two ① in some row, the right ① is sharing its box with a smaller number, so this row is not weakly increasing from left to right, a contradiction to the fact that T' is semistandard.

It remains to assemble the puzzle from the tableau T by reversing the first half of the bijection. From bottom to top, add in beams of rhombi of the correct height

Semistandard. The lower left picture shows that $u' + t' \geq s' + q' \geq p' + m'$. This directly translates to the semistandard condition of T , where \textcircled{i} is treated as i .

Ballot. The lower right picture shows the final type of inequalities, whose interpretation is still slightly more complicated. Following the notation from the previous proof, we get $b + t \geq_s r + q$ as one of these inequalities. Let us see how this kind of inequalities interact with the ballot condition. Let w be an initial segment of $\text{row}(T)$. As an example, let us compare the number of 2s and 3s. We may as well extend w with some more 3s without adding 2s. For example, suppose w ends between the 2s and 3s of row 2. There are at least as many (uncircled) 2s as (uncircled) 3s in w if and only if $b + t \geq r + q$. If there is a $\textcircled{2}$ between the 2s and 3s of row 2, the incremented erasure of w would have an extra 3. Therefore we must have $b + t \geq_s r + q$. Other requirements of the ballot condition all amount to inequalities of this type.

This establishes one direction of the bijection. As before, reversing the bijection and proving correctness is straight-forward, so we omit the details.

4D. Bijection between puzzles and tableaux. Rather than repeat similar proofs over and over, we present in table form the inequalities that can be read off from puzzles and their corresponding interpretations in both skew and \oplus tableaux rules.

For \blacktriangle , like for \blacklozenge , we let $x' = x + 1$ if the added tile is above the x -beam; otherwise $x' = x$. For \blacktriangledown and \blacklozenge , replace “above” in the definition above with “below.” Consequently, u', s', p', h' are undefined for \blacktriangledown and \blacklozenge .³ As before, $x \geq_z y$ is a shorthand for $x \geq y + z' - z$.

We first redescribe \blacklozenge rules in Table 1 to help orient the reader.

The inequalities for \blacklozenge , shown in Table 2, are very similar to those for \blacklozenge . The main difference is seen in the last rows of the tables. Consider the semistandard condition of the skew rule. While the inequality $a \geq_u t$ dictates that $\textcircled{1}$ in row 1 is to be written in the box *before* the 1s corresponding to u , the inequality $a \geq_t t$ instead dictates that $\textcircled{1}$ in row 2 is to be written in the box *after* the 1s corresponding to t . Similarly, for the \oplus rule’s ballot condition, the erasure is not incremented. The other difference is marked with (\blacktriangledown) due to \blacklozenge being upside down. We see that the limited condition arises naturally in the \oplus rule. Its counterpart in the skew rule is that the shape ν/λ cannot be enlarged by adding corners.

As compared to \blacklozenge , the inequalities for \blacktriangledown (Table 3) look quite different on the surface. However, it turns out we are essentially swapping the skew and \oplus rules with each other. Indeed, the only other difference is that \blacktriangledown , being upside down,

³The \blacktriangledown and \blacklozenge are “upside down” in the sense that they replace the upside down 1-triangle \blacktriangledown . Heuristically, since there are fewer opportunities to use these tiles, their corresponding set-valued tableaux have no option to fill a larger shape and circle tableaux have no \textcircled{i} in row i . The rules in the tables where this manifests itself are marked with (\blacktriangledown) .


	ν/λ	$\mu \oplus \lambda$
$\nu_1 - \lambda_1 = u$ $\nu_2 - \lambda_2 = s + t$ $\nu_3 - \lambda_3 = p + q + r$ $\nu_4 - \lambda_4 = h + m + n + o$	Shape: \textcircled{i} takes no space set-valued	Content: ignore \textcircled{i}
$\mu_1 = u' + t' + r' + o'$ $\mu_2 = s' + q' + n'$ $\mu_3 = p' + m'$ $\mu_4 = h'$	Content: $\textcircled{i} \mapsto i$	Shape: \textcircled{i} takes a box
$u' \geq s' \geq p' \geq h'$ $u' + t' \geq s' + q' \geq p' + m'$ $u' + t' + r' \geq s' + q' + n'$	Ballot: $\textcircled{i} \mapsto i$	Semistandard: $\textcircled{i} \mapsto i$
$a \geq_u t, \quad b \geq_t r, \quad c \geq_r o, \quad d \geq_o 0$ $b + t \geq_s r + q, \quad c + r \geq_q o + n, \quad d + o \geq_n 0$ $c + r + q \geq_p o + n + m, \quad d + o + n \geq_m 0$ $d + o + n + m \geq_h 0$	Semistandard: \textcircled{i} in previous box shape becomes ν/λ^-	Ballot: keep only last \textcircled{i} $\textcircled{i} \mapsto i + 1$

Table 1.  rules.


	ν/λ	$\mu \oplus \lambda$
$\nu_1 - \lambda_1 = u$ $\nu_2 - \lambda_2 = s + t$ $\nu_3 - \lambda_3 = p + q + r$ $\nu_4 - \lambda_4 = h + m + n + o$	Shape: \textcircled{i} takes no space set-valued	Content: ignore \textcircled{i}
$\mu_1 = u + t' + r' + o'$ $\mu_2 = s + q' + n'$ $\mu_3 = p + m'$ $\mu_4 = h$	Content: $\textcircled{i} \mapsto i$	Shape: \textcircled{i} takes a box no \textcircled{i} in row i (\blacktriangledown)
$u \geq s \geq p \geq h$ $u + t' \geq s + q' \geq p + m'$ $u + t' + r' \geq s + q' + n'$	Ballot: $\textcircled{i} \mapsto i$	Semistandard: $\textcircled{i} \mapsto i$
$a \geq_t t, \quad b \geq_r r, \quad c \geq_o o$ $b + t \geq_q r + q, \quad c + r \geq_n o + n$ $c + r + q \geq_m o + n + m$	Semistandard: \textcircled{i} in next box stay within shape (\blacktriangledown)	Ballot: keep only last \textcircled{i} $\textcircled{i} \mapsto i$

Table 2.  rules.













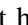


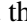
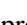

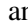
	ν/λ	$\mu \oplus \lambda$
$v_1 - \lambda_1 = u$ $v_2 - \lambda_2 = s + t'$ $v_3 - \lambda_3 = p + q' + r'$ $v_4 - \lambda_4 = h + m' + n' + o'$	Shape: \textcircled{i} takes a box no \textcircled{i} in row i ()	Content: $\textcircled{i} \mapsto i$
$\mu_1 = u + t + r + o$ $\mu_2 = s + q + n$ $\mu_3 = p + m$ $\mu_4 = h$	Content: ignore \textcircled{i}	Shape: \textcircled{i} takes no space set-valued
$u \geq_t s \geq_q p \geq_m h$ $u + t \geq_r s + q \geq_n p + m$ $u + t + r \geq_o s + q + n$	Ballot: keep only last \textcircled{i} $\textcircled{i} \mapsto i + 1$	Semistandard: \textcircled{i} in previous box stay within shape ()
$a \geq t', \quad b \geq r', \quad c \geq o'$ $b + t' \geq r' + q', \quad c + r' \geq o' + n'$ $c + r' + q' \geq o' + n' + m'$	Semistandard: $\textcircled{i} \mapsto i$	Ballot: $\textcircled{i} \mapsto i$

Table 3.  rules.

is less frequently usable, as denoted by () in two places. The first is the limited condition for the skew rule. However, any \textcircled{i} in row i would violate the ballot condition, so the limited condition need not be explicitly stated in [Theorem 3.6](#). The counterpart of the limited condition in the \oplus rule is that the shape cannot be enlarged by adding corners, as in the case of .

The close relation between  (shown in [Table 4](#)) and  is similar to that between  and . Indeed, one difference of  compared to  is that its erasure is not incremented and \textcircled{i} goes in the next box, just like . On the other hand, the other difference is that  does not have () restrictions,⁴ like . The lack of perfect symmetry is somewhat puzzling.

4E. Correspondence to coefficients. In the previous section, we presented in table form the relevant parts of the bijection between the four puzzle rules given in [Section 3B](#) and the eight tableau rules given in [Section 3C](#). What remains is to relate these to the coefficients defined in [Section 3A](#).

Buch [2002] proved [Theorem 3.5](#), establishing that the  rules count $c_{\lambda\mu}^v$. We proved above that the  rules count $d_{\lambda\mu}^v$. In the following two section, we establish  rules and  rules, respectively.

⁴So, in the \oplus rule, \textcircled{i} can be written in the next box, even protruding beyond the shape μ . However, if $\mu_2 = \mu_3$, say, the inequalities $s \geq_p p$ and $s + q \geq_m p + m$ prohibit $\textcircled{3}$ and $\textcircled{4}$, respectively, from protruding in row 3. As such, μ^+ is μ with some *outer corners* added.


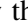
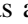
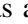
	v/λ	$\mu \oplus \lambda$
$v_1 - \lambda_1 = u'$ $v_2 - \lambda_2 = s' + t'$ $v_3 - \lambda_3 = p' + q' + r'$ $v_4 - \lambda_4 = h' + m' + n' + o'$	Shape: \textcircled{i} takes a box	Content: $\textcircled{i} \mapsto i$
$\mu_1 = u + t + r + o$ $\mu_2 = s + q + n$ $\mu_3 = p + m$ $\mu_4 = h$	Content: ignore \textcircled{i}	Shape: \textcircled{i} takes no space set-valued
$u \geq_s s \geq_p p \geq_h h$ $u + t \geq_q s + q \geq_m p + m$ $u + t + r \geq_n s + q + n$	Ballot: keep only last \textcircled{i} $\textcircled{i} \mapsto i$	Semistandard: \textcircled{i} in next box shape becomes μ^+
$a \geq t', \quad b \geq r', \quad c \geq o'$ $b + t' \geq r' + q', \quad c + r' \geq o' + n'$ $c + r' + q' \geq o' + n' + m'$	Semistandard: $\textcircled{i} \mapsto i$	Ballot: $\textcircled{i} \mapsto i$

Table 4.  rules.

4F. Proof of Theorem 3.7. Wheeler and Zinn-Justin [2017] proved Theorem 3.2, so we already know that the  rules count $\tilde{c}_{\lambda, \mu}^v$. Regardless, here we provide a simple calculation as a way to establish the  rules from the  rules, and that serves as an alternative proof to the result of Wheeler and Zinn-Justin.

By definition, we have

$$G_\mu \cdot G_1 = \sum_{\mu'} (-1)^{|\mu'| - |\mu| - 1} c_{\mu 1}^{\mu'} G_{\mu'}.$$

By Theorem 3.5, the coefficient $c_{\mu 1}^{\mu'}$ is 1 if μ' is μ with a positive number of outer corners added,⁵ and 0 otherwise. So

$$\begin{aligned} G_\lambda \cdot (G_\mu \cdot G_1) &= G_\lambda \sum_{\mu'} (-1)^{|\mu'| - |\mu| - 1} G_{\mu'} \\ &= \sum_{\mu'} (-1)^{|\mu'| - |\mu| - 1} \sum_v (-1)^{|v| - |\lambda| - |\mu'|} c_{\lambda, \mu'}^v G_v \\ &= - \sum_{v, \mu'} (-1)^{|v| - |\lambda| - |\mu|} c_{\lambda, \mu'}^v G_v, \end{aligned}$$

⁵Consider the shape $1 \oplus \mu$. The numbers filled in the lower box corresponds to the rows of μ'/μ .





where μ' runs over μ with a positive number of outer corners added. By definition, we have

$$\begin{aligned} \sum_v (-1)^{|v|-|\lambda|-|\mu|} \tilde{c}_{\lambda\mu}^v G_v &= G_\lambda \cdot G_\mu \cdot (1 - G_1) \\ &= \sum_v (-1)^{|v|-|\lambda|-|\mu|} c_{\lambda\mu}^v G_v + \sum_{v, \mu'} (-1)^{|v|-|\lambda|-|\mu|} c_{\lambda\mu'}^v G_v, \end{aligned}$$

so

$$\tilde{c}_{\lambda\mu}^v = c_{\lambda\mu}^v + \sum_{\mu'} c_{\lambda\mu'}^v.$$


By [Theorem 3.5](#), $\tilde{c}_{\lambda\mu}^v$ is the number of semistandard ballot set-valued tableaux of shape $\mu^+ \oplus \lambda$ and content v , where μ^+ is either μ or μ with a positive number of outer corners added, as desired.

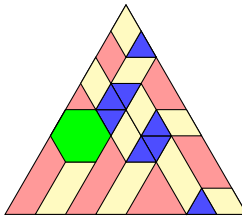
4G. Proof of Theorem 3.4. By [Theorem 3.3](#), it suffices to show a bijection between -puzzles with boundary $\Delta_{\lambda\mu}^v$ and -puzzles with boundary $\Delta_{\lambda'\mu'}^{v'}$. The bijection is simple: mirror the puzzle across a vertical line and swap the 0 and 1 labels. This is clearly an involution. Each of the original puzzle pieces is mapped to a valid puzzle piece. The  and  pieces are mapped to each other. The boundary is mapped from $\Delta_{\lambda\mu}^v$ to $\Delta_{\mu'\lambda'}^{v'}$.⁶ Finally, by definition, $d_{\lambda\mu}^v = d_{\mu\lambda}^v$, so we are done.


5. Final remarks

5A. Consider the example $\lambda = (2, 1)$, $\mu = (4, 2)$, and $v = (4, 3, 1)$. The skew tableau

	①	1	1
	2	2	
1			

corresponds to the -tiling



Since the shapes all fit in a 4×3 box, one might think $n = 7$ is sufficient side length for a puzzle. However, the  piece will protrude to the left of the puzzle with side length 7.

⁶Indeed, recall that the binary string of a partition λ corresponds to the boundary of the diagram of λ . Reversing the string rotates (the boundary of) the diagram by 180° . Swapping 0 and 1 in the string flips the diagram across the line $x = y$. Composing these two transformations flips the diagram across the line $x + y = 0$.

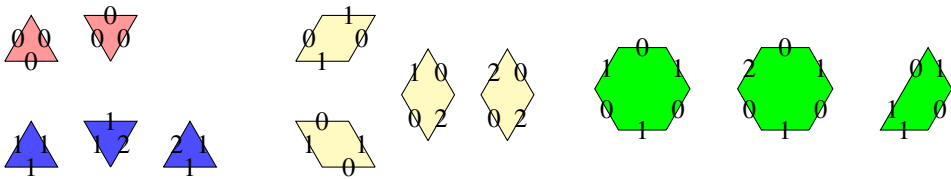
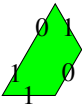



Figure 11. The complete set of tiles.

In [Theorem 3.3](#), we dealt with this issue by increasing the puzzle side length by one. More precisely, puzzles of side length $n + 1$ corresponds to using the standard ambient rectangle of size $(n - k) \times k$. So, to keep the side length of puzzles fixed at n , we must use a slightly narrower ambient rectangle of size $(n - 1 - k) \times k$ instead.


This is analogous for [Theorem 3.4](#). As we can see from the bijection outlined in its proof, we need the transposed partitions to fit inside a slightly narrower ambient rectangle, so the partitions themselves must fit inside a slightly shorter ambient rectangle of size $(n - k) \times (k - 1)$ instead.

5B. Another way to solve the protrusion issue outlined above is to add an additional trapezoid piece




as if to allow the hexagonal tile  to protrude to the left. (By the way things are set up, the hexagon never needs to protrude to the right or below.) However, we do not want this piece used elsewhere. So we must make some more modifications. [Figure 11](#) shows the complete set of tiles.

Consider the northeast–southwest slanting 1 edges. A 1-edge on the bottom-right side of pieces are now labeled with 2, so the new trapezoid piece cannot be used except at the left boundary. An old piece with a 1-edge on its top-left side must be duplicated, with a version for use at the left boundary and another for use in the interior.

Modification to  is similar.

5C. [Theorem 3.6](#) provides a skew tableau rule for calculating the K -theoretic Littlewood–Richardson coefficients $c_{\lambda\mu}^{\nu}$ using right circle tableaux. Pechenik and Yong [\[2017\]](#) give the same rule using *genomic* tableaux (definitions therein).

Theorem 5.1 (, [\[Pechenik and Yong 2017\]](#), K -theory, skew version). *The coefficient $c_{\lambda\mu}^{\nu}$ is the number of semistandard ballot genomic tableaux of shape ν/λ and content μ .*

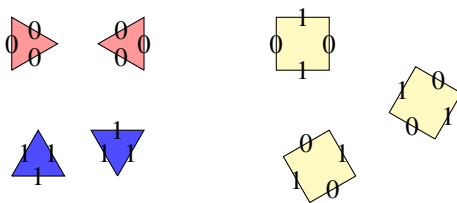


Figure 12. Mosaic version of the Knutson–Tao–Woodward tiles.

These two rules are virtually identical, as there is a simple bijection between right circle tableaux and genomic tableaux. Indeed, let a semistandard ballot right circle tableau of shape ν/λ and content μ be given. By semistandardness, the boxes filled with i and \textcircled{i} form a horizontal strip. From left to right, rewrite these as i_1, i_2, i_3 , and so on. Whenever \textcircled{i} is encountered, the *next* subscript used is the same as the current subscript. By ballotness, the rightmost i in the tableau is not circled, so this rule is well-formed. It is easy to see that this yields a semistandard genomic tableau of the same shape and content. One can also check that the tableau is ballot.

Conversely, given a semistandard ballot genomic tableau, the boxes filled with i_j for a fixed i form a horizontal strip. From left to right, circle an entry if its subscript is the same as the next one. Erase all subscripts. The correctness of this bijection is straightforward and left as exercise to the reader.

Example 5.2. The structure constant $c_{(2,1),(2,1)}^{(4,2,1)}$ is computed by the circle tableaux

$\begin{array}{ c c c c } \hline & & 1 & 1 \\ \hline & 2 & & \\ \hline \textcircled{1} & & & \\ \hline \end{array}$	$\begin{array}{ c c c c } \hline & & 1 & 1 \\ \hline & \textcircled{1} & & \\ \hline 2 & & & \\ \hline \end{array}$	$\begin{array}{ c c c c } \hline & & 1 & 1 \\ \hline & 2 & & \\ \hline \textcircled{2} & & & \\ \hline \end{array}$
---	---	---

and by the corresponding genomic tableaux

$\begin{array}{ c c c c } \hline & & 1_1 & 1_2 \\ \hline & 2_1 & & \\ \hline 1_1 & & & \\ \hline \end{array}$	$\begin{array}{ c c c c } \hline & & 1_1 & 1_2 \\ \hline & 1_1 & & \\ \hline 2_1 & & & \\ \hline \end{array}$	$\begin{array}{ c c c c } \hline & & 1_1 & 1_2 \\ \hline & 2_1 & & \\ \hline 2_1 & & & \\ \hline \end{array}$
---	---	---

5D. Purbhoo [2008] introduced mosaics, a useful variation of puzzles. These pieces do not need edge labels. Instead, edges labeled with 0 are rotated 30° anticlockwise. Below, the edge labels have been retained for clarity. Figure 12 shows the mosaic version of the ordinary Knutson–Tao–Woodward puzzle pieces.

Figure 13 shows the mosaic version of the four additional K -theoretic tiles. Note that the four tiles have the same geometric shape.

Acknowledgements

We are grateful to Allen Knutson and Joel Lewis for helpful conversations. We thank the anonymous referee for careful reading and useful suggestions. Pylyavskyy is partially supported by NSF grant DMS-1351590 and Sloan Fellowship. Yang is partially supported by NSF RTG grant NSF/DMS-1148634.

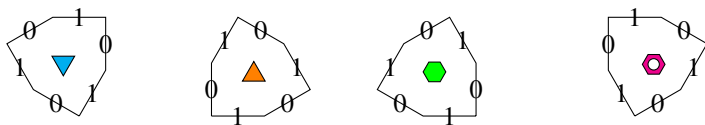


Figure 13. Mosaic version of the four additional K -theoretic tiles.

References

- [Buch 2002] A. S. Buch, “A Littlewood–Richardson rule for the K -theory of Grassmannians”, *Acta Math.* **189**:1 (2002), 37–78. [MR](#) [Zbl](#)
- [Fomin and Kirillov 1995] S. Fomin and A. N. Kirillov, “Grothendieck polynomials and the Yang–Baxter equation”, pp. 183–189 in *Formal power series and algebraic combinatorics* (New Brunswick, NJ, 1994), edited by L. J. Billera, Amer. Math. Soc., Providence, RI, 1995. [MR](#)
- [Fulton 1984] W. Fulton, *Intersection theory*, Ergebnisse der Mathematik (3) **2**, Springer, 1984. [MR](#) [Zbl](#)
- [Hazewinkel 1978] M. Hazewinkel, *Formal groups and applications*, Pure and Appl. Math. **78**, Academic Press, New York, 1978. [MR](#) [Zbl](#)
- [Knutson and Tao 1999] A. Knutson and T. Tao, “The honeycomb model of $GL_n(\mathbb{C})$ tensor products, I: Proof of the saturation conjecture”, *J. Amer. Math. Soc.* **12**:4 (1999), 1055–1090. [MR](#) [Zbl](#)
- [Knutson et al. 2004] A. Knutson, T. Tao, and C. Woodward, “The honeycomb model of $GL_n(\mathbb{C})$ tensor products, II: Puzzles determine facets of the Littlewood–Richardson cone”, *J. Amer. Math. Soc.* **17**:1 (2004), 19–48. [MR](#) [Zbl](#)
- [Lam and Pylyavskyy 2007] T. Lam and P. Pylyavskyy, “Combinatorial Hopf algebras and K -homology of Grassmannians”, *Int. Math. Res. Not.* **2007**:24 (2007), art. id. rnm125. [MR](#) [Zbl](#)
- [Lascoux and Schützenberger 1982] A. Lascoux and M.-P. Schützenberger, “Structure de Hopf de l’anneau de cohomologie et de l’anneau de Grothendieck d’une variété de drapeaux”, *C. R. Acad. Sci. Paris Sér. I Math.* **295**:11 (1982), 629–633. [MR](#) [Zbl](#)
- [Lenart and Zainoulline 2017] C. Lenart and K. Zainoulline, “A Schubert basis in equivariant elliptic cohomology”, *New York J. Math.* **23** (2017), 711–737. [MR](#) [Zbl](#)
- [Manivel 2001] L. Manivel, *Symmetric functions, Schubert polynomials and degeneracy loci*, SMF–AMS Texts and Monographs **6**, Amer. Math. Soc., Providence, RI, 2001. [MR](#) [Zbl](#)
- [Pechenik and Yong 2017] O. Pechenik and A. Yong, “Genomic tableaux”, *J. Algebraic Combin.* **45**:3 (2017), 649–685. [MR](#) [Zbl](#)
- [Purbhoo 2008] K. Purbhoo, “Puzzles, tableaux, and mosaics”, *J. Algebraic Combin.* **28**:4 (2008), 461–480. [MR](#) [Zbl](#)
- [Stanley 1999] R. P. Stanley, *Enumerative combinatorics, II*, Cambridge Studies in Adv. Math. **62**, Cambridge Univ. Press, 1999. [MR](#) [Zbl](#)
- [Vakil 2006] R. Vakil, “A geometric Littlewood–Richardson rule”, *Ann. of Math.* (2) **164**:2 (2006), 371–421. [MR](#) [Zbl](#)
- [Wheeler and Zinn-Justin 2017] M. Wheeler and P. Zinn-Justin, “Littlewood–Richardson coefficients for Grothendieck polynomials from integrability”, *J. Reine Angew. Math.* (online publication September 2017).
- [Zinn-Justin 2016] P. Zinn-Justin, *Puzzle/mosaic/Littlewood–Richardson tableau 4D viewer*, 2016, Available at <http://www.lpthe.jussieu.fr/~pzinn/puzzles>.

Received April 3, 2018. Revised March 3, 2019.

PAVLO PYLYAVSKYY
DEPARTMENT OF MATHEMATICS
UNIVERSITY OF MINNESOTA
MINNEAPOLIS
UNITED STATES

ppylyavs@umn.edu

JED YANG
DEPARTMENT OF MATHEMATICS AND COMPUTER SCIENCE
BETHEL UNIVERSITY
ST PAUL, MN
UNITED STATES

jed-yang@bethel.edu

PACIFIC JOURNAL OF MATHEMATICS

Founded in 1951 by E. F. Beckenbach (1906–1982) and F. Wolf (1904–1989)

msp.org/pjm

EDITORS

Don Blasius (Managing Editor)
Department of Mathematics
University of California
Los Angeles, CA 90095-1555
blasius@math.ucla.edu

Matthias Aschenbrenner
Department of Mathematics
University of California
Los Angeles, CA 90095-1555
matthias@math.ucla.edu

Daryl Cooper
Department of Mathematics
University of California
Santa Barbara, CA 93106-3080
cooper@math.ucsb.edu

Jiang-Hua Lu
Department of Mathematics
The University of Hong Kong
Pokfulam Rd., Hong Kong
jhlu@maths.hku.hk

Paul Balmer
Department of Mathematics
University of California
Los Angeles, CA 90095-1555
balmer@math.ucla.edu

Wee Teck Gan
Mathematics Department
National University of Singapore
Singapore 119076
matgwt@nus.edu.sg

Sorin Popa
Department of Mathematics
University of California
Los Angeles, CA 90095-1555
popa@math.ucla.edu

Paul Yang
Department of Mathematics
Princeton University
Princeton NJ 08544-1000
yang@math.princeton.edu

Vyjayanthi Chari
Department of Mathematics
University of California
Riverside, CA 92521-0135
chari@math.ucr.edu

Kefeng Liu
Department of Mathematics
University of California
Los Angeles, CA 90095-1555
liu@math.ucla.edu

Jie Qing
Department of Mathematics
University of California
Santa Cruz, CA 95064
qing@cats.ucsc.edu

PRODUCTION

Silvio Levy, Scientific Editor, production@msp.org

SUPPORTING INSTITUTIONS

ACADEMIA SINICA, TAIPEI
CALIFORNIA INST. OF TECHNOLOGY
INST. DE MATEMÁTICA PURA E APLICADA
KEIO UNIVERSITY
MATH. SCIENCES RESEARCH INSTITUTE
NEW MEXICO STATE UNIV.
OREGON STATE UNIV.

STANFORD UNIVERSITY
UNIV. OF BRITISH COLUMBIA
UNIV. OF CALIFORNIA, BERKELEY
UNIV. OF CALIFORNIA, DAVIS
UNIV. OF CALIFORNIA, LOS ANGELES
UNIV. OF CALIFORNIA, RIVERSIDE
UNIV. OF CALIFORNIA, SAN DIEGO
UNIV. OF CALIF., SANTA BARBARA

UNIV. OF CALIF., SANTA CRUZ
UNIV. OF MONTANA
UNIV. OF OREGON
UNIV. OF SOUTHERN CALIFORNIA
UNIV. OF UTAH
UNIV. OF WASHINGTON
WASHINGTON STATE UNIVERSITY

These supporting institutions contribute to the cost of publication of this Journal, but they are not owners or publishers and have no responsibility for its contents or policies.

See inside back cover or msp.org/pjm for submission instructions.

The subscription price for 2019 is US \$490/year for the electronic version, and \$665/year for print and electronic.
Subscriptions, requests for back issues and changes of subscriber address should be sent to Pacific Journal of Mathematics, P.O. Box 4163, Berkeley, CA 94704-0163, U.S.A. The Pacific Journal of Mathematics is indexed by [Mathematical Reviews](#), [Zentralblatt MATH](#), PASCAL CNRS Index, [Referativnyi Zhurnal](#), [Current Mathematical Publications](#) and [Web of Knowledge \(Science Citation Index\)](#).

The Pacific Journal of Mathematics (ISSN 1945-5844 electronic, 0030-8730 printed) at the University of California, c/o Department of Mathematics, 798 Evans Hall #3840, Berkeley, CA 94720-3840, is published twelve times a year. Periodical rate postage paid at Berkeley, CA 94704, and additional mailing offices. POSTMASTER: send address changes to Pacific Journal of Mathematics, P.O. Box 4163, Berkeley, CA 94704-0163.

PJM peer review and production are managed by EditFLOW[®] from Mathematical Sciences Publishers.

PUBLISHED BY



mathematical sciences publishers

nonprofit scientific publishing

<http://msp.org/>

© 2019 Mathematical Sciences Publishers

PACIFIC JOURNAL OF MATHEMATICS

Volume 303 No. 2 December 2019

Polarization, sign sequences and isotropic vector systems	385
GERGELY AMBRUS and SLOAN NIETERT	
L^p -operator algebras with approximate identities, I	401
DAVID P. BLECHER and N. CHRISTOPHER PHILLIPS	
The center of a Green biset functor	459
SERGE BOUC and NADIA ROMERO	
On the boundedness of multilinear fractional strong maximal operators with multiple weights	491
MINGMING CAO, QINGYING XUE and KÔZÔ YABUTA	
Embedding and compact embedding for weighted and abstract Sobolev spaces	519
SENG-KEE CHUA	
A pro- p group with infinite normal Hausdorff spectra	569
BENJAMIN KLOPSCH and ANITHA THILLAISUNDARAM	
Invariant connections and PBW theorem for Lie groupoid pairs	605
CAMILLE LAURENT-GENGOUX and YANNICK VOGLAIRE	
Random Möbius groups, I: Random subgroups of $\mathrm{PSL}(2, \mathbb{R})$	669
GAVEN MARTIN and GRAEME O'BRIEN	
Puzzles in K -homology of Grassmannians	703
PAVLO PYLYAVSKYY and JED YANG	
Linearly dependent powers of binary quadratic forms	729
BRUCE REZNICK	
Stability of the existence of a pseudo-Einstein contact form	757
YUYA TAKEUCHI	